Terra Nova
December 2015, Volume 27 Issue 6 Pages 467-478
https://doi.org/10.1111/ter.12181
https://archimer.ifremer.fr/doc/00287/39833/

Segmentation and kinematics of the North America-Caribbean plate boundary offshore Hispaniola

Leroy Sylvie [1,*], Ellouz-Zimmermann Nadine [2], Corbeau Jordane [1], Rolandone Frederique [1], Mercier De Lepinay Bernard [3], Meyer Bertrand [1], Momplaisir Roberte [4], Granja Bruna Jose-Luis [5], Battani Anne [2], Baurion Celine [1], Burov Evgueni [1], Clouard Valerie [6], Deschamps Remy [3], Gorini Christian [1], Hamon Youri [3], Lafosse Manfred [1], Leonel Jottin [7], Le Pourhiet Laetitia [1], Llanes Estrada Pilar [5], Loget Nicolas [1], Lucazeau Francis [6], Pillot Daniel [2], Poort Jeffrey [1], Tankoo Kevin R. [8], Cuevas Jose-Luis [9], Alcaide Jose-Fernando [9], Poix Claude Jean [10], Munoz-Martin Alfonso [5], Mitton Serge [11], Rodriguez Yamil [7], Schmitz Julien [2], Seeber Leonardo [12], Carbo-Gorosabel Andres [5], Munoz Santiago [13]

[1] Univ Paris 06, Univ Paris 04, CNRS UMR 7193, ISTEP, F-75005 Paris, France.
[2] IFPEnergies Nouvelles, Rueil Malmaison, France.
[3] Univ Nice Sophia Antipolis, CNRS, Geoazur, Valbonne, France.
[4] Univ Etat Haiti, Port Au Prince, Haiti.
[5] Univ Complutense Madrid, Madrid, Spain.
[6] IPGP, Observ Volcanol & Sismol Martinique, Fort De France, Martinique.
[7] Anamar, Santo Domingo, Dominican Rep.
[8] Univ W Indies, Dept Geog & Geol, Mona Kingston 7, Jamaica.
[9] CENAIS, Santiago De Cuba, Cuba.
[10] BME, Port Au Prince, Haiti.
[11] Semanah, Port Au Prince, Haiti.
[12] Lamont Doherty Earth Observ, Palisades, NY USA.
[13] Serv Geol Nacl, Santo Domingo, Dominican Rep.

* Corresponding author : Sylvie Leroy, email address : sylvie.leroy@upmc.fr

Abstract :

We explored the submarine portions of the Enriquillo–Plantain Garden Fault zone (EPGFZ) and the Septentrional–Oriente Fault zone (SOFZ) along the Northern Caribbean plate boundary using high-resolution multibeam echo-sounding and shallow seismic reflection. The bathymetric data shed light on poorly documented or previously unknown submarine fault zones running over 200 km between Haiti and Jamaica (EPGFZ) and 300 km between the Dominican Republic and Cuba (SOFZ). The primary plate-boundary structures are a series of strike-slip fault segments associated with pressure ridges, restraining bends, step overs and dogleg offsets indicating very active tectonics. Several distinct segments 50–100 km long cut across pre-existing structures inherited from former tectonic regimes or bypass recent morphologies formed under the current strike-slip regime. Along the most recent trace of the SOFZ, we measured a strike-slip offset of 16.5 km, which indicates steady activity for the past ~1.8 Ma if its current GPS-derived motion of 9.8 ± 2 mm a−1 has remained stable during the entire Quaternary.

1 – Introduction

Following the 2010 Mw 7.0 Haiti earthquake, an international effort was initiated to investigate the corresponding fault system and to constrain both the individual fault slip rates and their seismic history. Such an effort depends critically on knowledge of the detailed geometry of the fault system delineating the northern boundary of the Caribbean domain (Fig. 1). The Caribbean plate is currently moving eastward relative to North America and the plate motion is accommodated along a complex, 200 km-wide deformed zone, the Northern Caribbean plate Boundary (NCarB). The NCarB is a seismogenic zone extending over 3000 km along the northern edge of the Caribbean Sea (Fig. 1) and a deforming region that includes two large strike-slip fault systems, the Septentrional-Oriente fault zone (SOFZ) in the north and the Enriquillo-Plantain-Garden fault zone (EPGFZ) in the south (Mann *et al.*, 1991; Calais and De Lépinay, 1995). The SOFZ extends from the Mid Cayman spreading center, initiated 50 Ma ago (Leroy *et al.*, 2000), runs along the Southern coast of Cuba to cut across the northern Hispaniola (Calais and Mercier de Lépinay, 1989; Mann *et al.*, 1998). The EPGFZ, the prolongation to the east of Jamaica of the Walton fault, cuts across the Southern Peninsula in Haiti and dies out eastwards in the vicinity of the Muertos trough south of Hispaniola, delimiting the Gonâve microplate (DeMets and Wiggins-Grandison, 2007) (Fig. 1). Between the two strike-slip systems, the middle to late Eocene East Cayman margin is described offshore Jamaica (Leroy *et al.*, 1996) and the early Miocene to Present collisional wedge of Haiti, well-described onshore (Pubellier *et al.*, 2000), continues offshore in the Gonâve Gulf (Figs. 1 and 2).

Destructive earthquakes are reported along the NCarB both onshore and offshore (Ali *et al.*, 2008; Fig. 1). The most recent historical earthquakes known to have hit Northern Hispaniola are the 1842 event in Haiti and the 1562 event in Dominican Republic (Prentice *et al.*, 1993). Both events are commonly ascribed to the offshore portion of the Septentrional fault because paleosismological studies show that no surface rupture has occurred on the onshore Septentrional fault in central Dominican Republic in the last 800 years (Prentice *et al.*, 2003). Recent studies of historical earthquake accounts (ten Brink et *al.*, 2011; Bakun *et al.*, 2012) that have nonetheless assigned historical earthquakes to the onshore strike-slip faults remain challenged by the available paleosismological studies (Prentice *et al.*, 2013). The 6-12 mm/yr late Holocene slip rate of the Septentrional fault derived from the paleoseismological restoration (Prentice *et al.*, 2003) appears in agreement with the rate of 9.8 ±2 mm/yr computed from GPS along the Septentrional fault (Benford et al., 2012, Fig.1). Historical events reported for southern Hispaniola are commonly ascribed to the Hispaniola onshore portion of the EPGFZ (Ali et al., 2008). The source of the 2010 Haiti earthquake that remains uncertain (Bilham, 2010; Calais *et al.*, 2010; Prentice *et al.*, 2010; Mercier de Lépinay *et al.*, 2011, Douilly *et al.*, 2013) demonstrates the uncertainty inherent in the assignment of historical events to particular fault segments in the absence of contemporary observations of surface rupture or paleoseismic data. Benford *et al.* (2012) computed a 6.8 ±1 mm/yr GPS-derived horizontal slip rate for the EPGFZ but the short-term geological slip rate is unknown.

Offshore and onshore investigations were performed soon after the 2010 earthquake in the vicinity of Port-au-Prince to search for the source fault of this event (Hayes *et al.*, 2010; Prentice *et al.*, 2010; McHugh *et al.*, 2011; Mercier de Lépinay *et al.*, 2011). Here we report the results of two systematic offshore surveys of the NCarB from Cuba to Hispaniola and from Jamaica to Haiti and our analysis aimed at deciphering the segmentation of both fault systems. The marine geophysical data we collected (swath bathymetry from Haiti-sis and Norcaribe cruises, 1.8-5.3 kHz sub-bottom profiles and seismic reflection from Haiti-sis cruise) allow us to characterize the detailed geometry and kinematics of these two fault systems as well as to image the most recent cumulative fault trace disrupting the sea-bottom.

2 – Geometry and segmentation of the strike-slip fault systems

Multibeam bathymetry data reveal the geometry of the active submarine fault systems between Cuba and Haiti for the SOFZ, and between Jamaica and the Southern Peninsula of Haiti for the EPGFZ (Fig. 2). The faults we characterize as active bear by sharp scarps disrupting the sea-bottom and affect the shallowest unconsolidated sediments on the seismic profiles with suitable resolution to image the surficial sediments. Older faults bear significantly degraded scarps and the faults reported inactive do not disrupt the uppermost seismic units on the high-resolution seismic profiles. Active fault traces are very well preserved, especially the youngest strike-slip cumulative fault scarps that imprint the submarine landscape (Figs. 3, 4). The active fault system is remarkably linear and comprises a single strand along much of its length (Figs. 3, 4). Both fault systems display notable bends in their strikes. The strike of the SOFZ changes from N88°E to N100°E at 20°N and 72°50'W, south of Tortue Island (Fig. 3) and that of EPGFZ changes from N78°E to about EW west of Southern peninsula at 18°18'N and 74°30'W (Fig. 4). The fault segmentation, key information for seismic hazard assessment (e.g.; Wells and Coppersmith, 1994), can be defined on the basis of morphological and structural discontinuities such as fault bends and small jogs.

Along the active trace of the SOFZ, four distinct overlapping segments can be mapped from west to east. The western 90 km-long segment, segment 1 on Figure 3, runs offshore Cuba eastward to the Punta Caleta high, from 75°W to 74°05W. From 74°10W to 73°03W, a second 125 km-long segment bends 10° clockwise near longitude 73°40W, changing strike from N80°E to N90°E and traverses the no longer active Windward Passage Deep pull-apart. From 73°25W to 72°25W, a third 100 km-long segment trends N95°E west of the south Tortue Island bend and N100°E east of the bend. A fourth 100 km-long segment also trends N100°E and runs from east of Tortue Island eastward to the Dominican Republic (segment 4 in Fig. 3).

Along the EPGFZ, we interpret three distinct, overlapping, offshore segments on the basis of structural discontinuities (Fig. 4). Each segment has a clear morphologic imprint on the seafloor. From west to east, the eastern Jamaican segment corresponds to the offshore continuation of the Plantain Garden Fault described in Jamaica (Burke *et al.*, 1980; Mann *et al.*, 1985; Koehler *et al.*, 2013). The offshore portion of the eastern Jamaican segment is 25 km-long. The boundary between the Eastern Jamaican segment and the Western segment is defined by a left stepover at longitude 75°58'W (Fig. 4). The Western segment, about 70 km long, is associated with horsetail structures near the left step (Fig. 5) and traverses the 2800 m-deep Morant basin. Midway across the basin the active fault trace bisects a small compressional push-up (Fig. 5) and continues eastward to longitude 75°20'W. The Central segment (75°20'W to 75°10"W) is about 50 km long and overlaps the western segment for about 25 km. North-dipping thrusts, a few km apart of and sub-parallel to the central segment occur south of the main fault along most of its length (Fig. 4, 6). The eastern segment extends from 75°10'W, where a series of thrusts splay off the main strike-slip trace, to 74°33'W. The distance between the strike-slip trace and the thrust traces increases eastwards to reach a maximum of 15 km in the eastern Matley basin. The boundary between the 40 km-long eastern segment and the western Haitian segment is marked by a 2 km left-stepover, with both segments overlapping by 20 km. The western Haitian segment continues onshore Southern peninsula of Haiti along the base of a south-facing cumulative fault scarp (Figs. 1 and 4).

3. Fault kinematics, offset morphologies and slip-rate estimate

3.1 – Southern system - EPGFZ

Young submarine morphologies offset by strike-slip faults are rare because passive markers are unusual on the seafloor or because any such passive markers, if present, are commonly buried by sedimentation. This is the case for the EPGFZ and one has to rely on unambiguous kinematic indicators to assess the fault motion, such as in the Morant basin where the western and central segments overlap (Figs. 4 and 6). There, nearby the western tip of the central segment, *en echelon* pressure ridges testify for a primary left-lateral motion (Figs. 6 a,b). The *en echelon* ridges are well-expressed on the seafloor over a length of 7-8 km (Fig. 6b). An extensional horsetail splay by the left step-over between the western tip of the western segment and the eastern tip of the Jamaican segment also attests to left-lateral motion (Fig. 5). The regularly spaced normal faults branch from the master fault to the north where the western and Jamaican segments of the EPGFZ step-over. Further east, on the floor of the Morant basin, the fault cuts across a prominent structure obvious both on the reflectivity image and on the bathymetric map. A superficial analysis may induce doubt regarding the sense of motion of the EPGFZ, as it shows an apparent right-lateral offset (Fig. 6c). However, a more careful analysis reveals the presence of a restraining bend on the master fault that is associated with left-lateral motion (Fig. 5). In the Gobi Altai region such features have been extensively described along gentle bends of the main strike-slip system (Bayasgalan *et al.*, 1999; Cunningham, 2007). The local restraining bend along the EPGFZ is now bypassed by the main strike-slip fault in agreement with a primary strike-slip motion at depth.

The Navassa basin, located on the central segment at the longitude of 75°15’W, is a 40-km-long and 5km-wide asymmetric basin (Fig. 4). Sub-bottom seismic profiles (1.8-5.3 kHz) show that this basin is deeper along the master strike-slip fault (Fig. 4 lower right inset). Such asymmetric basins are typically formed along strike-slip fault systems (Ben-Avraham and ten Brink, 1989; Mann *et al.*, 1995; Cunningham, 2007; Mann, 2007; Smit *et al.*, 2008). The sedimentary sequence infilling the Navassa basin is thicker towards the north, where the present-day depocentre is located along the main strike-slip fault (lower right inset of Fig. 4). A large landslide (4 by 4 km), possibly earthquake-induced, impinges on the southern flank of the Navassa ridge and moved southward within the Navassa basin (Fig. 4 upper right inset). Similar mass movement may present a source of tsunami for the nearby coast of Haiti and Jamaica (Hornbach *et al.*, 2010).

The EPGFZ cross cuts pre-existing morphologies and the current deformation stage is superimposed on older tectonic structures as depicted by the seismic section crossing the Morant basin (Fig. 7). The sediment layers have been tilted by the previous activity of a normal fault in a large half-graben similar to the ones identified in the northern Jamaica margin (Fig. 1; Leroy *et al.*, 1996). The overall sedimentary infill has been subsequently folded with unevenly distributed gentle folds and the final crosscutting by the EPGFZ is associated with very limited adjacent compressive structures.

3.2 – Northern fault system - SOFZ

We identified a notable exception to the lack of well-identified offset geomorphic features on the SOFZ at about 19°50'N-72°14'W. There, the course of a NS channel flowing northward veers abruptly to the west within the strike-slip furrow (Fig. 8, red arrows) and bends abruptly again to the north to cross the North Hispaniola Deformed Belt (Fig. 3a). The canyon is 400-800m deep and its downstream course incises a carbonate platform, which outcrops closely (<~20km) in Dominican Republic and Haiti (Calais *et al.*, 1992). In between the upstream and downstream courses, there is no significant canyon south of the fault. However, the upstream part of the channel faces another channel north of the fault (Fig. 8, green arrow) but the latter is beheaded at the fault precluding a former continuity of these channels as well as the piracy of the upstream course of the offset channel. Therefore the 16.5 km-long dogleg offset of the channel has been preserved (Fig. 8, red arrows).

A similar shift of a second canyon occurs toward the west, near the Tortue Island (Fig. 8). The corresponding offset is more difficult to assess because there are several possibilities of upstream courses (blue arrows on Fig. 8), the easternmost one pointing to a plausible offset of 16.5 km. The analysis of the bathymetric profiles (Fig. 9) confirms this estimate although we lack full multibeam bathymetry coverage of the shallow platform merging with the shore to verify that this largest offset does correspond to a large canyon merging onland with a significant river. The NGA nautical charts offshore Cap-Haitien and Tortue Island combined with the new dataset provide some candidates for the onshore source river system (Fig. 8).

In the western part of the SOFZ, the active fault trace crosses the Windward Passage Deep through the basin (Fig. 3; at the longitude of 73°50W). This 40 km-long, 10 km-wide and 3700 m-deep basin is described as an early Miocene pull-apart by Calais and De Lépinay (1995), and it is now cross-cut by the present trace of SOFZ (Fig. 3).

4 – Discussion and Conclusions

Our work brings to light a hitherto poorly known, 500km-long portion of the offshore active strike-slip fault systems of the North America-Caribbean plate boundary. The bathymetry and seismic data delineate multiple left-lateral, 50 to 100 km-long, strike-slip fault segments. The geometry of the active fault systems does not seem to be controlled by pre-existing tectonic features (rifted basin, folds). The lengths of the fault segments we have identified along both the EPGFZ and the SOFZ are capable of producing Mw ~7-7.7 earthquakes (e.g.; Wells and Coppersmith, 1994) that are likely to trigger prominent submarine landslides in the vicinity of Hispaniola similar to the one we highlight in Fig. 4.

Paleoseismic studies performed along the onshore SOFZ trace in Dominican Republic show that the most recent ground-rupturing earthquake occurred more than 800 years ago (Prentice *et al.*, 1993; Prentice *et al.*, 2003), suggesting the 1842 earthquake most likely occurred along the offshore segment documented here, in tune with the triggering of a tsunami at Cap Haïtien (Lander *et al.* 2002; Prepetit, 2008).

On the SOFZ, the 16.5 km dogleg offset of two canyons is not dated, nor is the limestone platform into which the canyons are incised, ruling out a direct determination of the geological slip-rate of the SOFZ. Based on the geology of adjacent coast we propose an estimate age of 2 Ma for the upper part of the carbonate platform which is reefal onshore (Villa Vasquez series; De Zoeten and Mann, 1991; Calais et al. 1992) and with a suggestive karstic morphology offshore (Fig. 8) indicating a low sea level and subaerially environments, respectively. The occurrence of stepped terraces along the northern wall fault implies the record of paleo-sealevels, a position above sea surface where waves action progressively erase the karstic terrain and a progressive uplift of the northeastern block relative to the southern one. Eastward wedge of stepped terraces indicates a variable uplift along the fault coeval with the activity of the SOFZ for significant time periods (Fig. 8). If the 9.8 ±2 mm/yr slip rate derived from the GPS (Benford *et al.*, 2012) has remained constant, at least during the whole Quaternary, the 16.5 km offset would yield an age of ~1.8 Ma for its inception. Interestingly, this age matches that estimate of the upper part of the carbonate platform and of the recent uplift of the Septentrional Cordillera in the northern Dominican Republic which is bounded on its southern edge by the onshore portion of the SOFZ (Calais and Mercier de Lépinay, 1989) and of the northwestern Cordillera of Haiti (Bowin, 1975; Nagle *et al.*, 1979; Prentice *et al.*, 1993; Mann *et al.*, 1995; 1998). ~ 1.8 Ma is the likely age for the uplift above sea-level of the erased karst block, the Tortue island and further west, the windward passage sill (Calais and De Lépinay, 1995). Channels offset and vertical movements are probably indicative of a southward plate boundary shift along SOFZ (around 2 Ma) that could be driven either by the Bahamas-Hispaniola collision (Dolan *et al*. 1998; Mann *et al*. 2002) or deeper processes such as Slab Edge Push (Van Bethem *et al*. 2014). Our study does not allow deciphering between the importance of the two mechanisms. Nonetheless the geometry and segmentation of the offshore SOFZ and EPGFZ and the primary strike-slip motion highlighted along the offshore portion EPGFZ are key information for seismic hazard assessment, stress-transfer calculations and GPS-derived kinematic models.

Acknowledgments

We thank Captain Moimeaux, crews and technicians from L'Atalante (IFREMER/GENAVIR). We are indebt from French Embassies in Haiti, Bruno Asseray, and Cuba, Aurelie Nogues, Oliver Tenes. The local authorities are also thanked, Daysarih Tapanes Robau from CITMA, Claude Prépetit from BME, D. Boisson and J. Jadotte from UEH. We wish to thank captain and crew of the R/V Sarmiento de Gamboa and technicians of the UTM (Norcaribe cruise funded by the SMIS (CGL2010-17715). We also thank UPMC and IFPEN for solving several administrative issues. We acknowledge constructive comments by three reviewers and are grateful to the Associate Editor and Editor for the efficient processing of the manuscript.

References

Ali, S.T., Freed, A.M., Calais, E., Manaker, D.M., and McCann, W.R., 2008. Coulomb stress evolution in Northeastern Caribbean over the past 250 years due to coseismic, postseismic and interseismic deformation. Geophysical Journal International **174**, 904-918.

Bakun, W.H., Flores, C.H. and ten Brink, U.S., 2012. Significant Earthquakes on the Enriquillo Fault System, Hispaniola, 1500-2010: Implications for Seismic Hazard *Bulletin of the Seismological Society of America*, **102**, 18-30.

Bayasgalan, A., Jackson, J., Ritz, J.F., and Carretier, S., 1999. `Forebergs', flower structures, and the development of large intra- continental strike-slip faults: the Gurvan Bogd fault system in Mongolia. Journal of Structural Geology **21**, 1285-1302.

Ben-Avraham, Z., and ten Brink, U.S., 1989. Transverse faults segmentation of basins within the Dead Sea Rift. Journal of African Earth Science **8**, 603-610.

Benford, B., DeMets, C., and Calais, E., 2012. GPS estimates of microplate motions, northern Caribbean: evidence for a Hispaniola microplate and implications for earthquake hazard. Geophysical Journal International **191**, 481-490.

Bilham, R., 2010. Structural geology: Invisible faults under shaky ground. Nature Geosci **3**, 743-745.

Bowin, C., 1975. The Geology of Hispaniola. Springer, 501-552.

Burke, K., Grippi, J., and Sengör, C., 1980. Neogene structures in Jamaica and tectonic style of the northern Caribbean plate boundary zone. Journal of Geology **88**, 375-386.

Calais, E., and Mercier de Lépinay, B., 1989. Des données nouvelles sur la Cordillère Septentrionale de République Dominicaine : ses relations avec la limite de plaques décrochante nord Caraïbe. C. R. Acad. Sci. Paris **309**, 409-415.

Calais, E., and de Lépinay, B.M., 1991. From transtension to transpression along the northern Caribbean plate boundary off Cuba: implications for the Recent motion of the Caribbean plate. Tectonophysics 186, 329-350.

Calais, E., Mercier De Lepinay, B., Saint-Marc, P., et al., 1992. La limite de plaques décrochante Nord Caraïbe en Hispaniola: évolution paléogéographique et structurale cénozoïque Bull. Soc. géol. France, 163, 309-324.

Calais, E., and De Lépinay, B., 1995. Strike-slip tectonic processes in the northern Caribbean between Cuba and Hispaniola (Windward Passage). Marine Geophysical Researches **17**, 63-95.

Calais, E., Freed, A., Mattioli, G., et al. 2010. Transpressional rupture of an unmapped fault during the 2010 Haiti earthquake. Nature Geosci **3**, 794-799.

Corbeau, J., Rolandone, F., Leroy, S., Mercier De Lepinay, B., Meyer B. and Ellouz-Zimmerman N., 2014. The Northern Caribbean Plate Boundary Offshore Hispaniola: Strike-slip and Compressive Tectonic Processes - AGU Fall meeting, San Francisco.

Cunningham, D., 2007. Structural and topographic characteristics of restraining bend mountain ranges of the Altai, Gobi Altai and easternmost Tien Shan. Geological Society, London, Special Publications **290**, 219-237.

Cunningham, W.D., and Mann, P., 2007. Tectonics of strike-slip restraining and releasing bends. Geological Society, London, Special Publications **290**, 1-12.

DeMets, C., and Wiggins-Grandison, M., 2007. Deformation of Jamaica and motion of the Gonâve microplate from GPS and seismic data. Geophysical Journal International **168**, 362-378.

de Zoeten, R. and Mann, P., 1991. Structural geology and Cenozoic tectonic history of the central Cordillera Septentrional, Dominican Republic (P. Mann, G. Draper and J.F. Lewis, eds), Boulder, 262, 265-279.

Dolan, J.-F., Mullins, H.T. and Wald, D., 1998. Active Tectonics of the north-central Caribbean: Oblique collision strain partitioning and opposing subducted slabs. In: *Active strike-slip and collisonal Tectonics of the Northern Caribbean plate boundary zone* (J.-F. Dolan and P. Mann, eds). Geological Society of America Special Papers, Boulder, Colorado, **326**, 1-62.

Granja Bruña, J.L., Carbó-Gorosabel, A., Llanes Estrada, P., et al., 2014. Morphostructure at the junction between the Beata ridge and the Greater Antilles island arc (offshore Hispaniola southern slope). Tectonophysics **618**, 138-163.

Hornbach, M.J., Braudy, N., Briggs, R.W., et al., 2010. High tsunami frequency as a result of combined strike-slip faulting and coastal landslides. Nature Geoscience **3**, 783-788.

Horsfield, W., and Robinson, E., 1974. Marine geology of the Jamaica Passage, Trans. 7th Caribb. Geol. Conf., pp. 103-107.

Koehler, R.D., Mann, P., Prentice, C.S., Brown, L., Benford, B., and Wiggins-Grandison, M., 2013. Enriquillo-Plantain Garden Fault Zone in Jamaica: Paleoseismology and Seismic Hazard. Bulletin of the Seismological Society of America **103**, 971-983.

Lander, J.F., Whiteside, L.S. and Lockridge, P.A., 2002. A brief history of tsunamis in the Carribean Sea *Sceince of Tsunami Hazards*, **20**, 57-94.

Leroy, S., Mercier de Lépinay, B., Mauffret, A., and Pubellier, M., 1996. Structure and tectonic evolution of the Eastern Cayman trough (Caribbean Sea) from seismic reflection data. Am. Ass. Petrol. Geol. Bull. **80**, 222-247.

Leroy, S., Mauffret, A., Patriat, P., and Mercier de Lépinay, B., 2000. An alternative interpretation of the Cayman trough evolution from a reidentification of magnetic anomalies. Geophys. J. Int. **141**, 539-557.

Mann, P., Draper, G., and Burke, K., 1985. Neotectonics of a strike-slipe restraining bend system, Jamaica. The society of Economic Paleontologists and Mineralogist **10**, 211-226.

Mann, P., Tyburski, S., and Rosencrantz, E., 1991. Neogene development of the Swan Islands restraining-bend complex, Caribbean Sea. Geology **19**, 823-826.

Mann, P., Taylor, F.W., Laurence Edwards, R., and Ku, T.-L., 1995. Actively evolving microplate formation by oblique collision and sideways motion along strike-slip faults: An example from the northeastern Caribbean plate margin. Tectonophysics **246**, 1-69.

Mann, P., Prentice, C.S., Burr, G., et al. 1998. Tectonic geomorphology and paleoseismology of the Septentrional fault system, Dominican Republic. In: *Active strike-slip and collisonal Tectonics of the Northern Caribbean plate boundary zone* (J.-F. Dolan and P. Mann, eds). Geological Society of America Special Papers, Boulder, Colorado, **326**, 63-123.

Mann, P., Calais, E., Ruegg, J.-C., et al., 2002. Oblique collision in the northeastern Caribbean from GPS measurements and geological observations *Tectonics*, **21**, 7-1-7-26.

Mann, P., 2007. Global catalogue, classification and tectonic origins of restraining- and releasing bends on active and ancient strike-slip fault systems. Geological Society, London, Special Publications **290**, 13-142.

Mann, P., DeMets, C., and Wiggins-Grandison, M., 2007. Toward a better understanding of the Late Neogene strike-slip restraining bend in Jamaica: geodetic, geological, and seismic constraints. Geological Society, London, Special Publications **290**, 239-253.

Mauffret, A. and Leroy, S., 1997. Seismic stratigraphy and structure of the Caribbean Igneous Province. Tectonophysics **283**, 61-104.

McHugh, C.M., Seeber, L., Braudy, N., *et al.* 2011. Offshore sedimentary effects of the 12 January 2010 Haiti earthquake. Geology **39**, 723-726.

Mercier de Lépinay, B., Deschamps, A., Klingelhoefer, F., et al., 2011. The 2010 Haiti earthquake: A complex fault pattern constrained by seismologic and tectonic observations. Geophysical Research Letters **38**, L22305; 22301-22317.

Nagle, F., Palmer, H.C., and Antonini, G.A., 1979. Hispaniola: Tectonic Focal Point of the Northern Caribbean. Three geologic studies in the Dominican Republic. Miami Geological society, 1-103.

Prentice, C.S., Mann, P., Taylor, F.W., Burr, G., and Valastro, S., 1993. Paleoseismicity of the North American-Caribbean plate boundary (Septentrional fault), Dominican Republic. Geology **21**, 49-52.

Prentice, C.S., Mann, P., Peña, L.R., and Burr, G., 2003. Slip rate and earthquake recurrence along the central Septentrional fault, North American–Caribbean plate boundary, Dominican Republic. Journal of Geophysical Research **108**, 2149.

Prentice, C.S., Mann, P., Crone, A.J., et al., 2010. Seismic hazard of the Enriquillo-Plantain Garden fault in Haiti inferred from palaeoseismology. Nature Geosci **3**, 789-793.

Prentice, C.S., Mann, P. and Peña, L.R., 2013. Comment on "Historical perspective on seismic hazard to Hispaniola and the northeast Caribbean region" by U. ten Brink et al *Journal of Geophysical Research: Solid Earth*, **118**, 1-4.

Prepetit, 2008. Tremblements de terre en Haiti: mythe ou réalité. In: *Le Matin*, Haiti.

Pubellier, M., Mauffret, A., Leroy, S., Vila, J.M., and Amilcar, H., 2000. Plate boundary readjustement in oblique convergence: Example of the Neogene of Hispaniola, Greater Antilles. Tectonics **19**, 630-648.

Smit, J., Brun, J.P., Cloetingh, S., and Ben-Avraham, Z., 2008. Pull-apart basin formation and development in narrow transform zones with application to the Dead Sea Basin. Tectonics **27**, 1-17.

ten Brink, U.S., Bakun, W.H. and Flores, C.H., 2011. Historical perspective on seismic hazard to Hispaniola and the northeast Caribbean region Journal of Geophysical Research, 116, B12318-12315.

van Benthem, S., Govers, R. and Wortel, R., 2014. What drives microplate motion and deformation in the northeastern Caribbean plate boundary region? *Tectonics*, **33**, 850-873.

Wells, D.L. and Coppersmith, K.J., 1994. New Empirical Relationships among Magnitude, Rupture Length, Rupture Width, Rupture Area, and Surface Displacement *Bulletin of the Seismological Society of America*, **84**, 974-1002.

Figures Captions

Figure 1: Tectonic map of the northern Caribbean plate boundary. Orange dots indicate the presumed epicenter of Mw>7 historical earthquakes from (Ali *et al.*, 2008), orange dashed lines indicate imprecisely localized historical earthquakes. Velocities in mm/yr reported from a block model incorporating the available GPS data (Benford *et al.*, 2012). The studied parts of the fault systems in this paper are outlined in red. Faults in black are from previous studies (Calais and de Lepinay et al 1989; Calais, E., and de Lepinay, B.M., 1991; Mann *et al.* 1995; 1998; Leroy *et al*. 1996 ; Mauffret and Leroy 1997; Granja Buna *et al*.2014; in Gulf of Gonave from Corbeau *et al*. 2014) **Inset:** Geodynamic map. NOAM: North American; CAR: Caribbean; GMP: Gonâve microplate. MCSC: Mid-Cayman spreading center; CT: Cayman trough; D.R.: Dominican Republic; NJAM: North Jamaican Margin; OFZ: Oriente Fault zone; EPGFZ: Enriquillo-Plantain Garden Fault zone; SFZ: Septentrional Fault zone; WFZ: Walton Fault zone; SDB: Santiago Deformed Belt; BPF: Bahamas platform; HsB: Haiti sub-basin; BR: Beata ridge; BF: Bunce Fault, BoF: Bowin Fault, MR: Mona rift.

Figure 2: 50 m resolution bathymetric map of the Hispaniola area from several cruises: Haiti-sis 1&2 (2012, 2013 on R/V L'Atalante), Norcaribe (2013 on R/V Sarmiento de Gamboa), Haiti-OBS (2010; R/V L'Atalante; (Mercier de Lépinay *et al.*, 2011)) and Seacarib 1 & 2 (1985, R/V Conrad; 1987, R/V J. Charcot; (Calais and De Lépinay, 1995; Leroy *et al.*, 1996; Mauffret and Leroy, 1997)). Rectangles with number locate the corresponding figures. Inset: Location of the cruises Haiti-OBS (orange); Seacarib 1 & 2 (purple); Norcaribe (green); Haiti-sis 1 & 2 (blue).

Figure 3: Bathymetric map of the Septentrional-Oriente fault zone (SOFZ) and tectonic interpretation. Fault segmentation inferred from distinct geometric fault complexities (fault bends and small jogs). W.P. Deep: Windward Passage Deep. Active fault segments are in red and inactive one or pre-existing structures from older tectonic events are in black. Onland Hispaniola the main rivers are shown in blue.

Figure 4: Bathymetric map of the southern system Enriquillo-Plantain Gardain Fault zone (EPGFZ) and tectonic interpretation (Lower panel). Active fault segments are in red while inactive or older ones are in black. The eastern Jamaican segment is the offshore continuity of the Plantain Garden Fault identified onland in Jamaica. The western Haitian segment is the prolongation of the Southern Peninsula fault observed in Haiti (faults are drawn in green onland). These segments are connected

by three hitherto unrecognized, western central and eastern offshore segments. J: Jamaica; H: Haiti. Lower right Inset is a subbottom seismic profile (1.8-5.6kHz) crossing the EPGFZ in the Navassa basin (grey line for location). Upper right inset is a close-up of the northern wall of the Navassa basin showing a large landslide (4x 4 km). The white dashed lines represents the scar of the mass failure and white arrows point to the corresponding deposits on the basin floor.

Figure 5: Upper panel: Bathymetric map of the western termination of the western segment of the EPGFZ. See figure 2 for location. Lower panel: Tectonic interpretation with extensional horsetail splay and restraining bend in the Morant basin. Note the very limited local shortening observed at the restraining bend ultimately bypassed by the most recent fault trace in the Morant basin, in agreement with the occurrence of recent releasing bend described onshore crosscut by the Haitian prolongation of the strike-slip fault system (i.e Clonard pull-apart (Fig. 1) (Mann *et al.*, 1995)).

Figure 6: a, 3D-view from the SW of the western offshore portion of the EPGFZ. Two overlapping segments with linear fault traces (black arrows), 3 km apart, cut across a pre-existing bathymetry. The dashed line indicates the location of the seismic profile on Fig. 7. b, Detailed bathymetry along the two parallel fault traces. The western segment to the north is highlighted by a narrow strike-slip furrow. The central segment to the south displays 1.5 km long, 150 m wide, and 15 m high *en echelon* pressure ridges. c, Reflectivity image of the active trace of the western segment ot the EPGFZ cutting across a prominent transpressive structure (restraining bend ; see Cunningham & Mann, 2007 for classification).

Figure 7: Migrated shallow seismic profile across the EPGFZ nearby the Morant basin and corresponding interpretation (upper panel). Red lines represent recent active trace of the EPGFZ, clearly identified on the profile. Other faults (black lines) are supposed to be active before and not during the very recent motion along the EPGFZ. A gentle compressive structure in the north of the EPGFZ is also crosscut by this seismic profile. Pre-existing southward-tilted series and syn-tectonic sequence are deformed before the recent motion along the active fault (Corbeau *et al.* 2014).

Figure 8: Map view of the offshore prolongation of the Septentrional Fault (labelled SOFZ), North of Haiti (see Figs 1 & 2 for location). Note the linearity of the fault trace and fault parallel canyon, and the downstream and upstream courses of two offset channels (large vertical arrows). Note the 16.5 km dogleg offset of the eastern canyon (red arrows) which upstream course faces a beheaded

channel north of the fault (oblique white arrow) and parallels a shallow canyon south of the fault (vertical orange arrow) For the western dogleg offset canyon, the downstream canyon is beheaded while the upstream feasible ones merge with the bottom of the fault parallel canyon. The size of the blue arrows south of the fault increases with that of the resulting offset, the biggest arrow pointing to the likely 16.5 km offset. The offset channels, 400-800m deep, incise a platform, presumably carbonated which outcrops in Dominican Republic (Calais *et al.*, 1992). North of the fault, large parts of the platform display a hummocky pattern with impressive swallow holes, which is suggestive of drowned karstic terrain. Stepped terraces may indicate a gradual uplift of the northeastern block relative to the southern wall fault. Onland present-day rivers are indicated (thicked lines are the major one) and NGA nautical charts available offshore Cap-Haitien and Tortue Island are used to draw two channels (brawn lines). Note that the large canyon (orange arrow) was already mapped on the nautical chart but appears unlikely for matching the red arrow canyon with our multibeam data.

Figure 9: a, Bathymetric profiles parallel to the fault projected on a vertical plane striking N100°E. Arrows are drawn as in fig. 8 and location of the profile is shown in the inset map. The downstream offset canyons are 400-800 m wide and 1600-1250 m deep while the downstream-beheaded channel to the east (oblique green arrow) is less incised. Minimum offset of the eastern channel, shown by the red arrows, is 16.5km. A smaller offset is ruled out by the absence, south of the fault, of any significant canyon between the upstream and downstream courses. A larger offset of 24 km (orange arrow) appears unlikely because, south of the fault, the next channel to the east with an appropriate width is less incised and too shallow to match the morphology of the downstream offset channel. b, The profile in the south of the fault (grey) has been displaced by 16.5 km to restore the offset of the canyon. Note also the restoration of the overall morphology with similar regional slopes on both side of the main canyon.

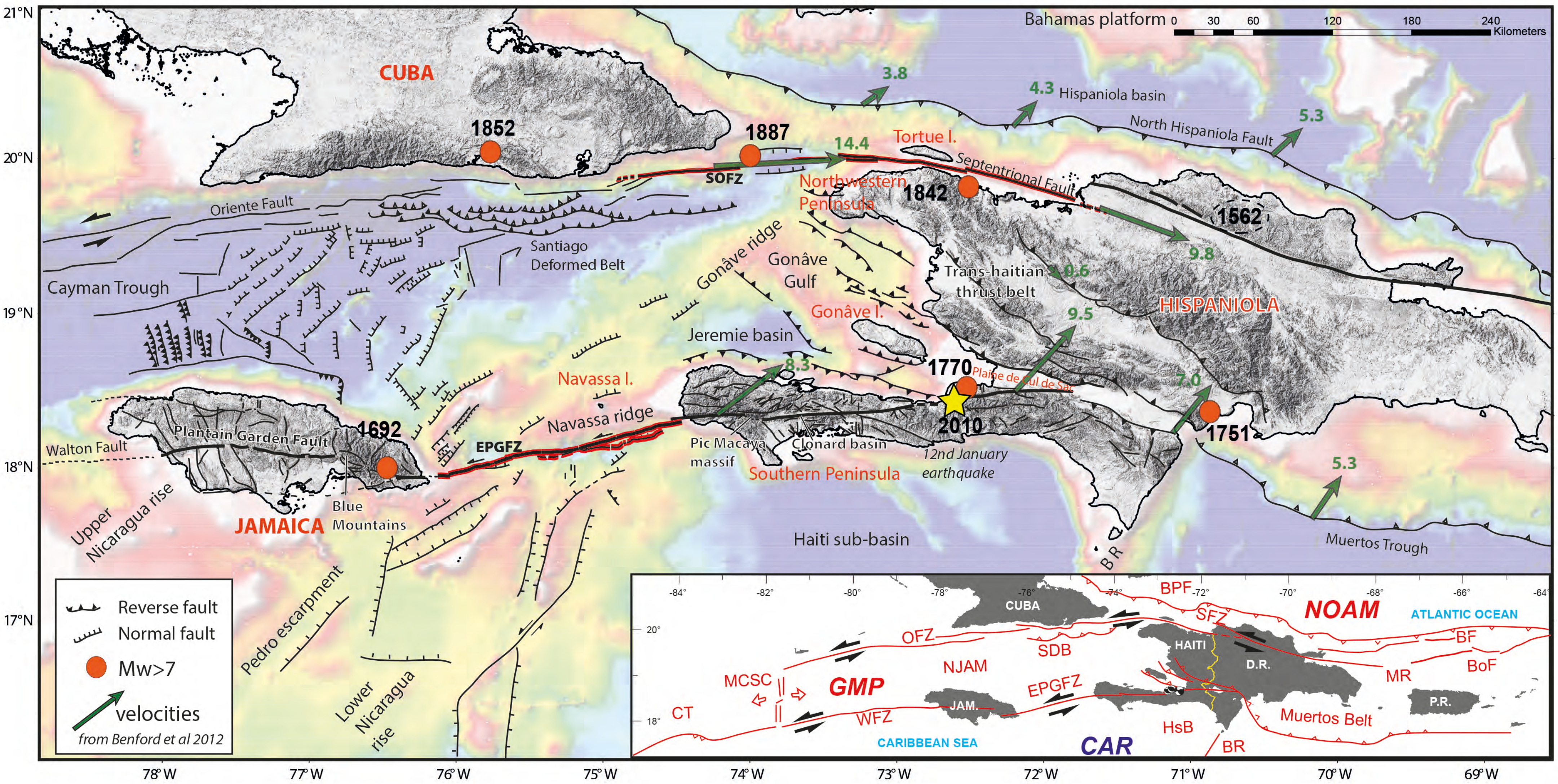

Bahamas platform
0 30 60 120 180 240 Kilometers
CUBA
1852
1887
SOFZ
14.4
3.8
4.3
Hispaniola basin
North Hispaniola Fault
5.3
Tortue I.
Septentrional Fault
Northwestern Peninsula
1842
1562
9.8
Oriente Fault
Santiago Deformed Belt
Cayman Trough
Gonâve ridge
Gonâve Gulf
Trans-haitian thrust belt
10.6
HISPANIOLA
Gonâve I.
9.5
Jeremie basin
8.3
1770
Plaine de Cul de Sac
7.0
1751
Navassa I.
Navassa ridge
2010
12nd January earthquake
Plantain Garden Fault
1692
EPGFZ
Walton Fault
Pic Macaya massif
Clonard basin
Southern Peninsula
5.3
Upper Nicaragua rise
JAMAICA
Blue Mountains
Haiti sub-basin
Muertos Trough
B R
Pedro escarpment
Lower Nicaragua rise
Reverse fault
Normal fault
Mw>7
velocities
from Benford et al 2012
21°N
20°N
19°N
18°N
17°N
78°W
77°W
76°W
75°W
74°W
73°W
72°W
71°W
70°W
69°W
BPF
SFZ
NOAM
ATLANTIC OCEAN
CUBA
HAITI
D.R.
OFZ
SDB
BF
MR
BoF
MCSC
GMP
NJAM
EPGFZ
CT
JAM.
WFZ
HsB
Muertos Belt
P.R.
CARIBBEAN SEA
CAR
BR

Fig 1

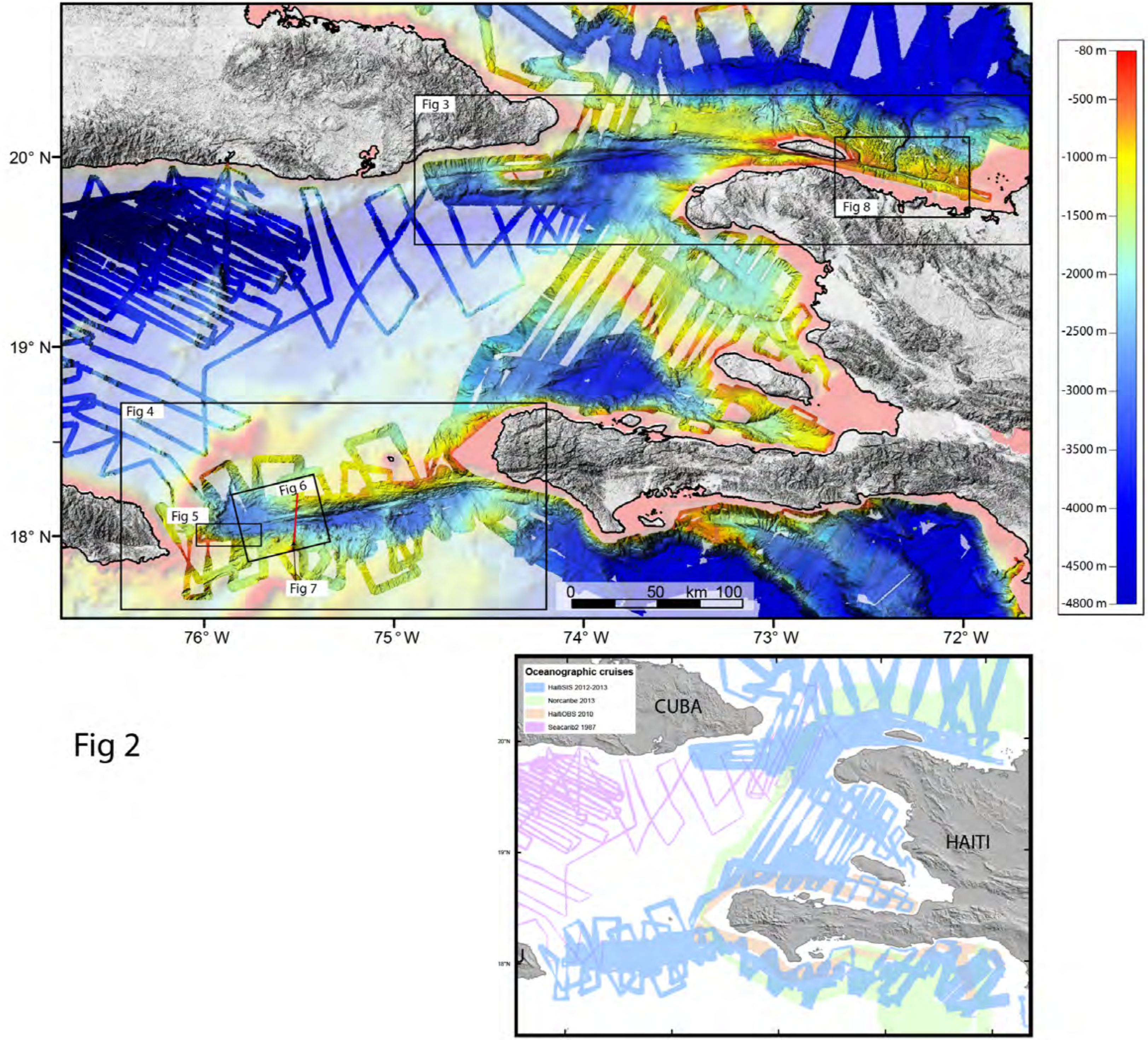
Fig 3
Fig 8
Fig 4
Fig 5
Fig 6
Fig 7
20° N
19° N
18° N
76° W
75° W
74° W
73° W
72° W
0
50
km
100
-80 m
-500 m
-1000 m
-1500 m
-2000 m
-2500 m
-3000 m
-3500 m
-4000 m
-4500 m
-4800 m
Oceanographic cruises
HaitiSIS 2012-2013
Norcaribe 2013
HaitiOBS 2010
Seacarib2 1987
CUBA
HAITI

Fig 2

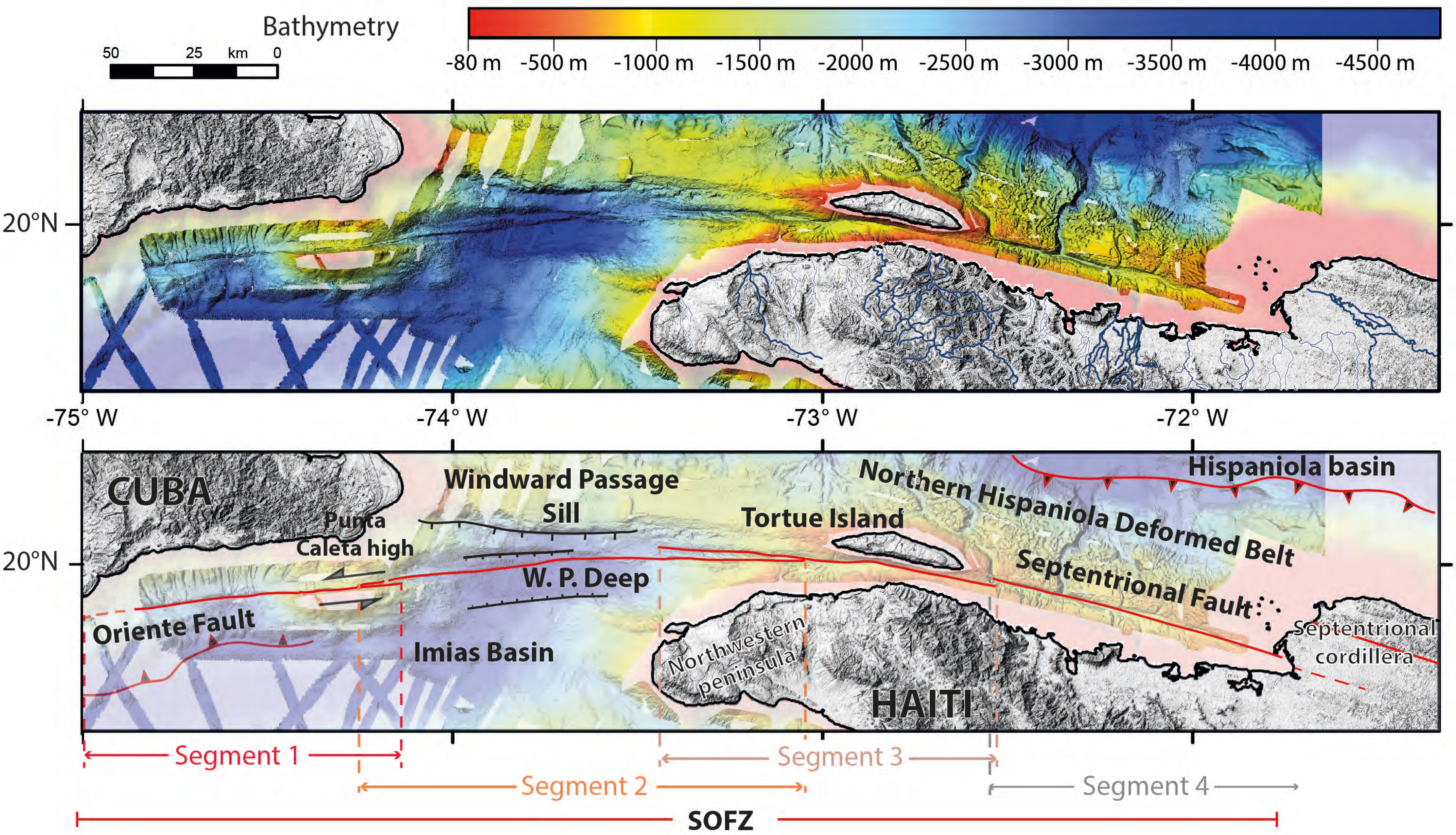

Bathymetry
50
25
km
0
-80 m
-500 m
-1000 m
-1500 m
-2000 m
-2500 m
-3000 m
-3500 m
-4000 m
-4500 m
20°N
-75° W
-74° W
-73° W
-72° W
CUBA
Windward Passage
Sill
Punta
Caleta high
W. P. Deep
Oriente Fault
Imias Basin
Tortue Island
Northern Hispaniola Deformed Belt
Hispaniola basin
Septentrional Fault
Septentrional
cordillera
Northwestern
peninsula
HAITI
Segment 1
Segment 2
Segment 3
Segment 4
SOFZ

Fig3

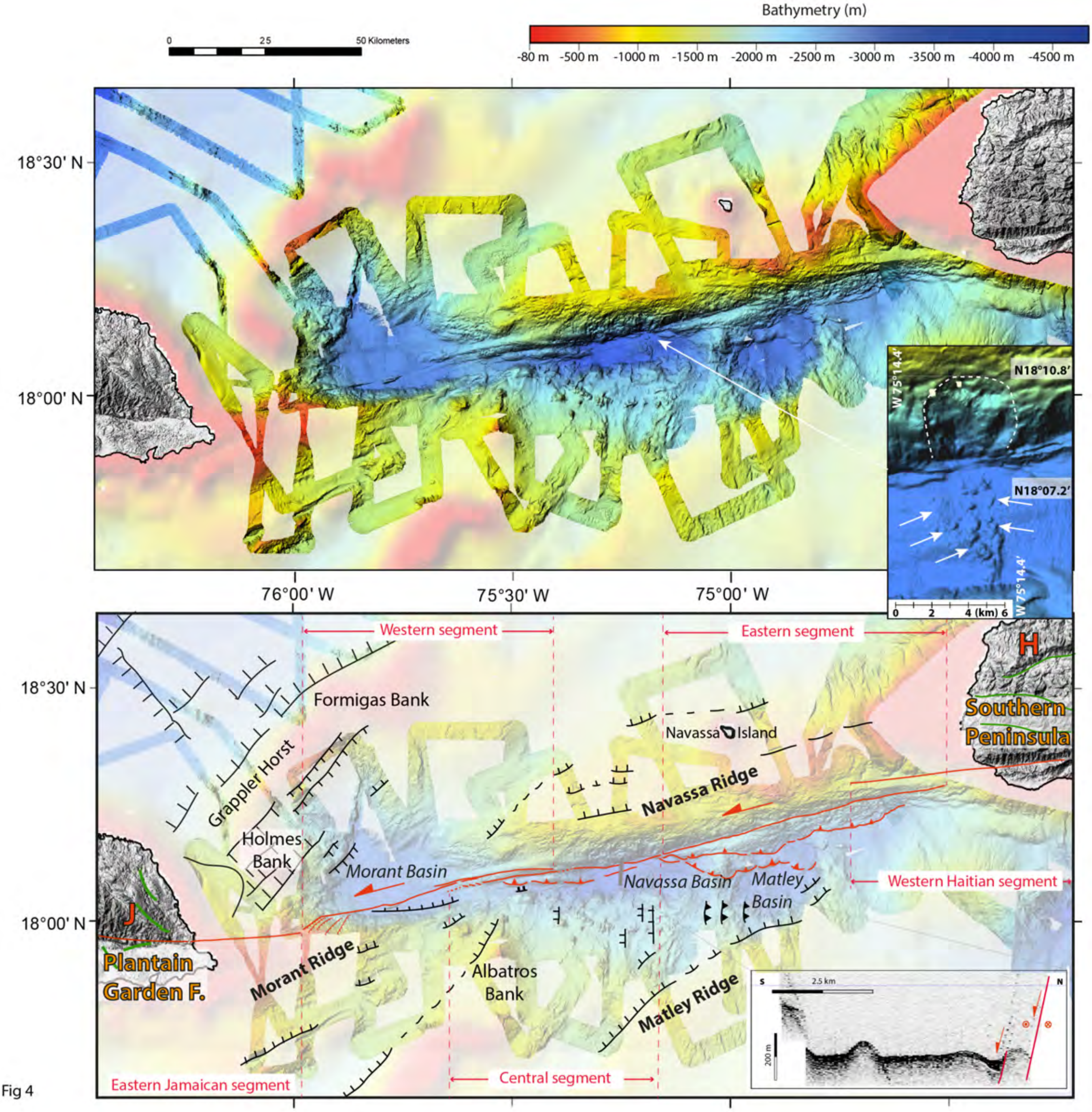

Bathymetry (m)
-80 m
-500 m
-1000 m
-1500 m
-2000 m
-2500 m
-3000 m
-3500 m
-4000 m
-4500 m
0
25
50 Kilometers
18°30' N
18°00' N
76°00' W
75°30' W
75°00' W
N18°10.8'
N18°07.2'
W 75°14.4'
0 2 4 (km) 6
Western segment
Eastern segment
Formigas Bank
Navassa Island
Grappler Horst
Navassa Ridge
Holmes Bank
Morant Basin
Navassa Basin
Matley Basin
Western Haitian segment
H
Southern Peninsula
J
Plantain Garden F.
Morant Ridge
Albatros Bank
Matley Ridge
Eastern Jamaican segment
Central segment
2.5 km
200 m
S
N

Fig 4

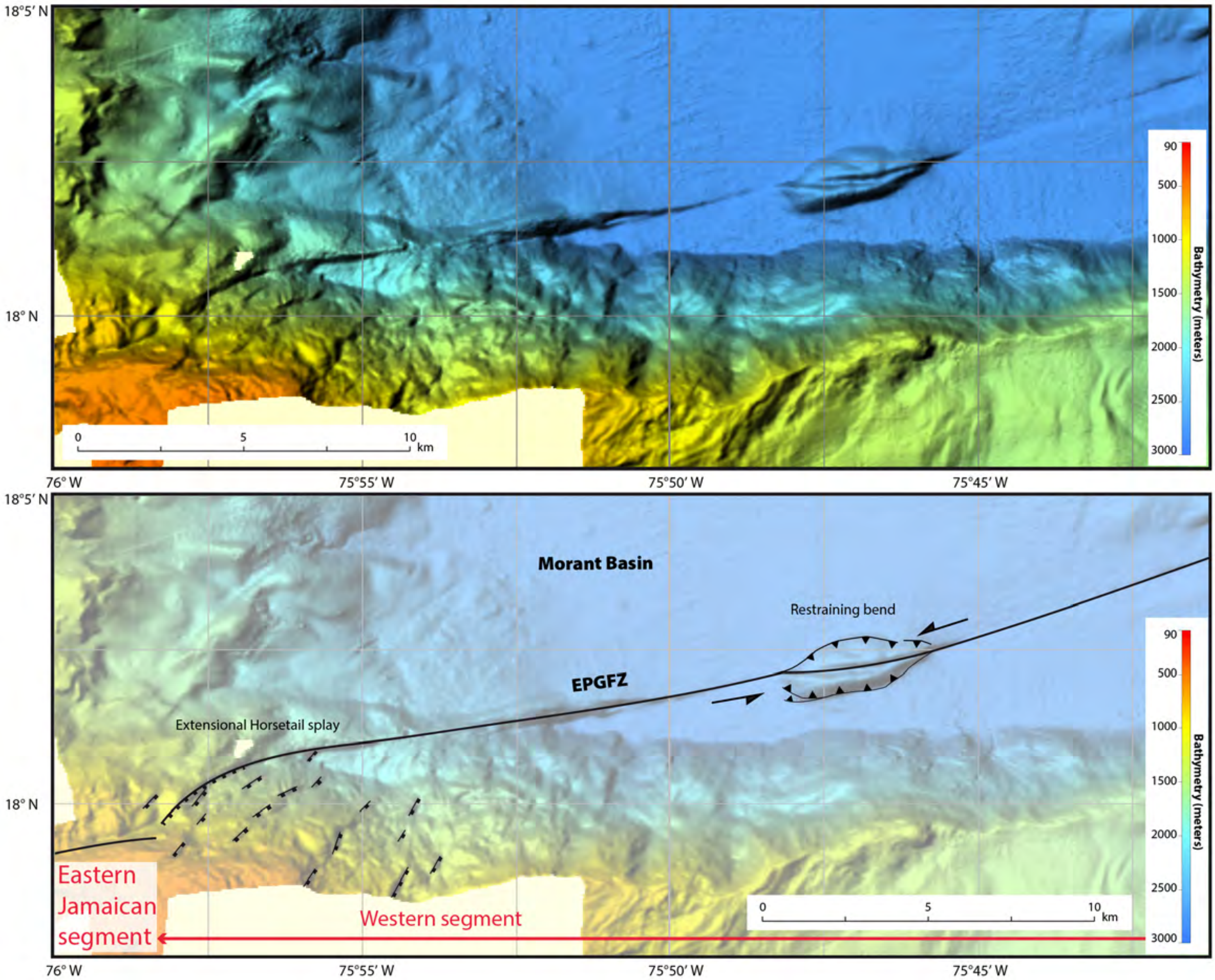
18°5′ N
18° N
0
5
10
km
90
500
1000
1500
2000
2500
3000
Bathymetry (meters)
76° W
75°55′ W
75°50′ W
75°45′ W
Morant Basin
Restraining bend
EPGFZ
Extensional Horsetail splay
Eastern
Jamaican
segment
Western segment

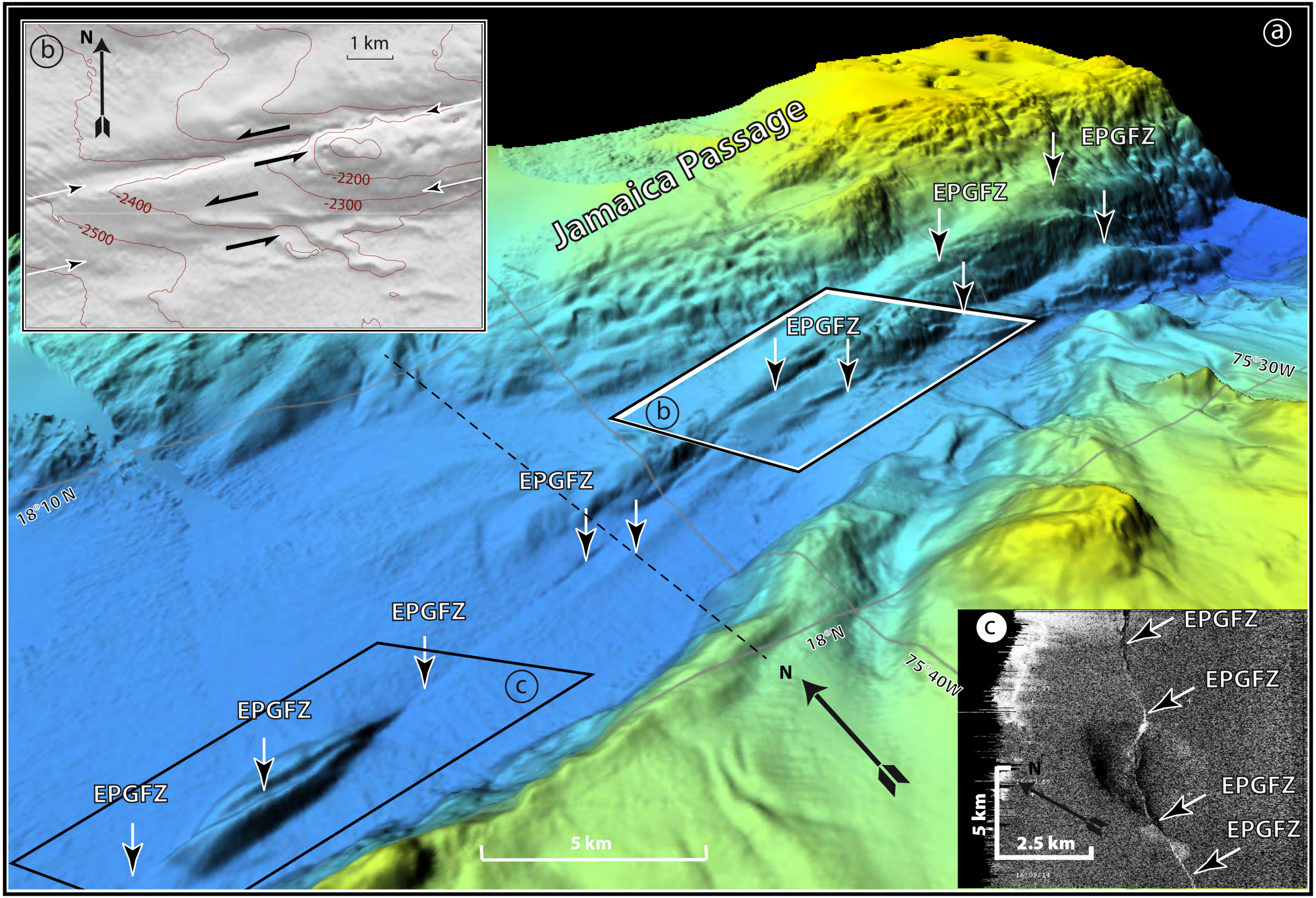
a
b
N
1 km
-2200
-2300
-2400
-2500
Jamaica Passage
EPGFZ
EPGFZ
EPGFZ
EPGFZ
EPGFZ
EPGFZ
EPGFZ
b
c
75°30W
75°40W
18°10 N
18°N
N
5 km
c
EPGFZ
EPGFZ
EPGFZ
EPGFZ
N
5 km
2.5 km

Fig 6

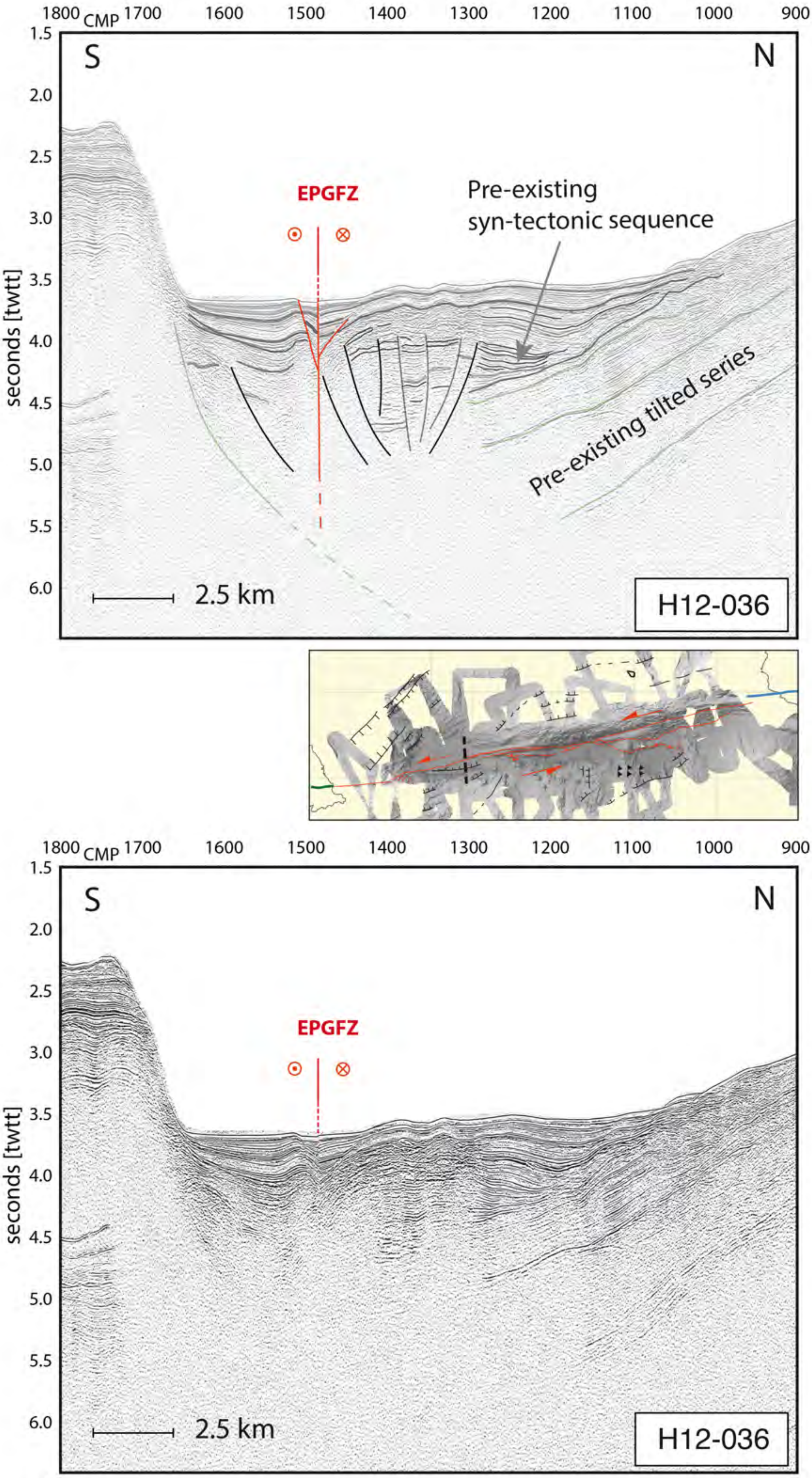
1800 CMP 1700 1600 1500 1400 1300 1200 1100 1000 900
1.5 2.0 2.5 3.0 3.5 4.0 4.5 5.0 5.5 6.0
seconds [twtt]
S
N
EPGFZ
Pre-existing
syn-tectonic sequence
Pre-existing tilted series
2.5 km
H12-036
1800 CMP 1700 1600 1500 1400 1300 1200 1100 1000 900
1.5 2.0 2.5 3.0 3.5 4.0 4.5 5.0 5.5 6.0
seconds [twtt]
S
N
EPGFZ
2.5 km
H12-036

Fig 7

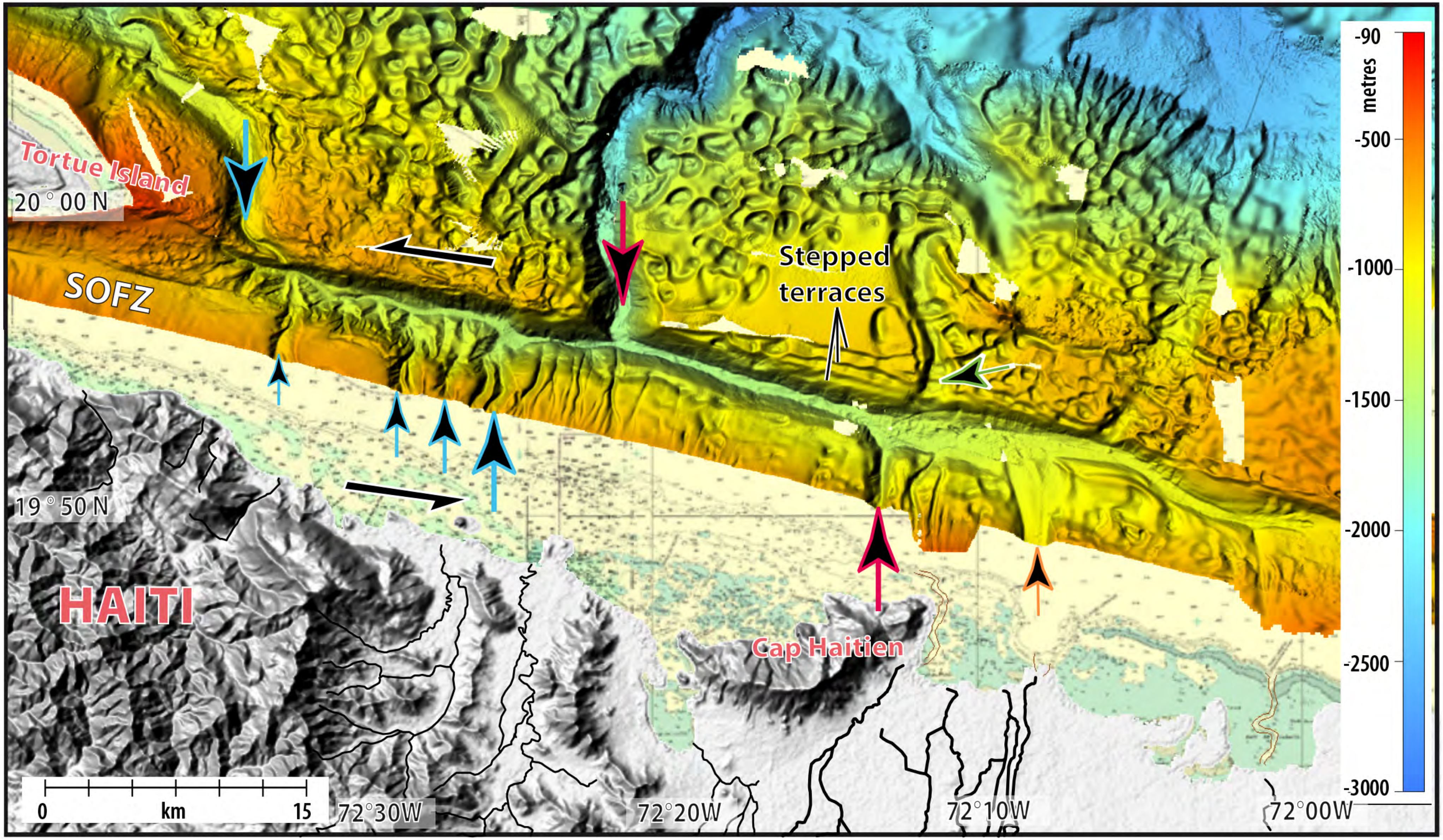

Tortue Island
20 ° 00 N
SOFZ
Stepped
terraces
19 ° 50 N
HAITI
Cap Haitien
0
km
15
72°30W
72°20W
72°10W
72°00W
-90
metres
-500
-1000
-1500
-2000
-2500
-3000

Figure 8

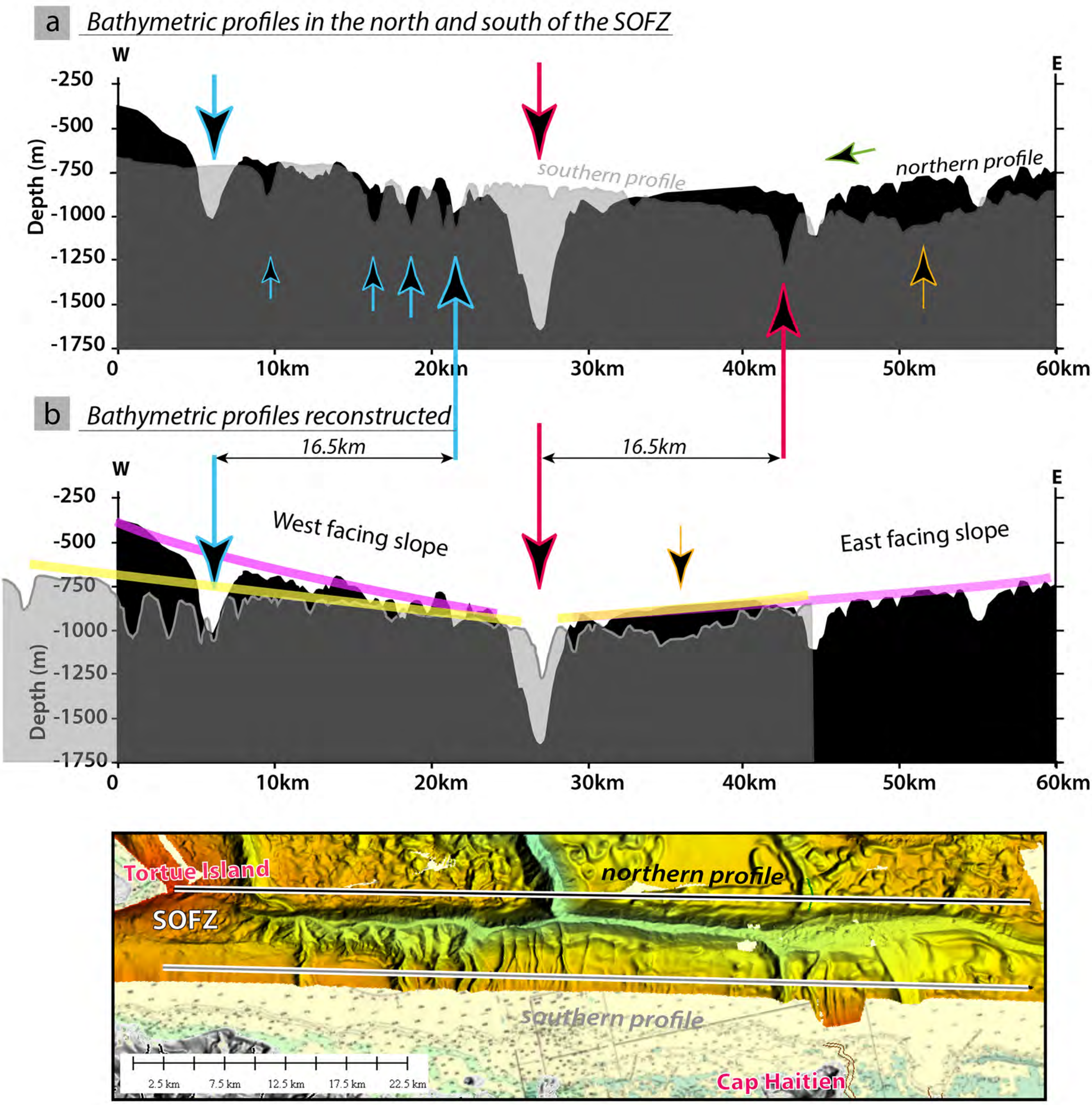
a
Bathymetric profiles in the north and south of the SOFZ
W
E
Depth (m)
-250
-500
-750
-1000
-1250
-1500
-1750
0
10km
20km
30km
40km
50km
60km
southern profile
northern profile
b
Bathymetric profiles reconstructed
16.5km
16.5km
West facing slope
East facing slope
Tortue Island
SOFZ
northern profile
southern profile
Cap Haitien
2.5 km
7.5 km
12.5 km
17.5 km
22.5 km

Figure 9